



# Welding of AMg4 aluminum alloy by applying ultrasonic vibrations

S. K. Sundukov

sergey-lefmo@yandex.ru

Moscow Automobile and Road Construction State Technical University (MADI), Moscow, 125319, Russia

The effects of applying ultrasonic vibrations in welding of AMg4 aluminum alloy are studied. The experimental studies in the considered conditions allowed finding the optimal amplitude of vibrations (9–10  $\mu\text{m}$ ). When ultrasound is applied to the molten pool, the liquid metal is subject to sound pressure, cavitation, and acoustic flows, which affects the crystallization parameters. The comparison of the microstructure of the welding zone shows a significantly reduced dendritic segregation when vibrations are applied. The weld joint obtained in the selected conditions has an increased strength and high plasticity.

**Keywords:** ultrasound, welding, vibrations, cavitation, microstructure, dendritic segregation.

## 1. Introduction

The primary disadvantage of fusion welding is uneven heat introduction into parts to be joined. This results in a cast structure of the melt and solidified weld metal. The transition over the melt boundary to the base metal is accompanied by changes in mechanical properties. Along with structural differences, welding issues also include residual stresses, welding deformations, and weld porosity [1].

To a great extent, these issues are found in welding aluminum structures. Due to high heat capacity and heat conductivity, it is required to increase heat introduction as compared to steel welding because up to 5% higher welding current is used. A strong overheating of the joint zone and a high expansion coefficient of aluminum cause a significant weld metal shrinkage when it solidifies, which results in high residual strains [2]. The high solubility of gases in melted aluminum increases the probability of gas pores during crystallization. Shrinkage of aluminum may also cause pores shaped as irregular micro-pores similar to micro-cracks [3].

Aluminum is susceptible to oxidation both in solid and liquid states. An oxide film formed on the solid material and  $\text{Al}_2\text{O}_3$  formed during welding have a melting temperature above the melting temperature of aluminum and are insoluble in liquid aluminum, prevent weld metal fusion with base metal, and form non-metallic inclusions in the weld [4].

One of the efficient methods to minimize the consequences of these drawbacks is ultrasonic treatment of metal in the molten state [5–8].

There are following methods of using ultrasonic vibrations during welding: applying vibrations to the electrode [9], applying vibrations to the non-consumable electrode [10], transferring vibrations to the gas burner body [11], transferring vibrations to non-weldable structural elements [12], using the arch as a source of ultrasonic radiation [13]. The studies using these methods can be found in overview paper [14].

A number of papers have been devoted to ultrasonic treatment of aluminum. In [15], ultrasound treatment of large ingots made of aluminum alloy 2324 was carried out. The resulted structure fully consists of spherical grains without dendritic branches. There is a cavitation effect for melt degassing — small hydrogen bubbles on the surface of oxides grow actively due to the effect of hydrogen rectified diffusion from the melt into a cavitation bubble. The bubbles are then fused reaching the size necessary to emerge on the surface.

Dong et al. [16] studied the joining of plates of aluminum alloy 5A06 with low-carbon galvanized steel Q235A by welding with a non-consumable electrode using filler 4047Al. The welding was overlap-type and an ultrasound vibration system was pressed to the aluminum plate 30 mm from the welding bath under its own weight. The temperature conditions of the welding were selected so as to melt aluminum without steel melting, which minimizes the formation of brittle intermetallics Al-Fe. As a result, the weld metal on the interface with steel has a significantly refined dendritic structure and there are almost no dendrites on the interface with aluminum. Microstructural changes are explained by cavitation that results in dispersion to dendrites and changes the nucleation conditions. The authors of Ref. [17] studied building-up on a plate made of aluminum alloy 2219 using filler wire ER2319 by welding with a non-consumable electrode. Ultrasound was regularly transmitted to the plate via a contact roller that was rolled over the plate 90 mm from the welding zone. This resulted in a weld with a periodical structure: during vibrations, the structure is refined and equiaxed grains are formed. The structural refinement leads to the micro-hardness of the weld metal increased to 8.5%. The proof testing of pure aluminum welding showed a decreased length of dendritic grains in the fusion zone. In [18], the microstructure of a joint made of aluminum alloy 2A14 containing about 4.5% copper was studied. Building-up was done by transmitting pulse ultrasound vibrations via the

gas burner body. The vibration frequency was 20 kHz; the pulse frequency was 50 Hz. Using this method increased the weld penetration, which is explained by an ultrasound standing field formed in the arc burning space that increases the frequency of plasma particles collision and imposes the arch heat emission. There is also a decreased grain size in the center of the weld metal by 30  $\mu\text{m}$  on average.

The results of studies on the influence of ultrasound effect on the heterogeneous formation of grains when welding with a non-consumable electrode 2195 Al-Li are presented in [19]. Vibrations with the frequency of 35 kHz were applied at a distance of 11 cm from the welding zone. Due to vibrations, the grains around the fusion zone changed from columnar to equiaxial ones. The primary mechanism was a temperature rise during nucleation.

Despite the positive results, the process has not yet found wide application. Additional studies are required to expand the range of materials and allow one to evaluate the effect of various modes of ultrasonic vibrations.

The present paper provides the results of studies on the effects of ultrasonic vibrations on welded elements in the case of semiautomatic welding of AMg4 alloy. The introduction of vibrations into the welding zone is selected because it can be done during the entire welding cycle, from molten pool formation to weld solidification.

## 2. Materials and Experimental Methods

### 2.1. Materials

During experimental studies, the base metal was aluminum alloy AMg4 that belongs to wrought, non-hardenable aluminum alloys used to produce semi-finished products by hot or cold forming that are widely applied in construction, aircraft and ship-building. This alloy grade was selected because the material has high weldability properties. The initial workpiece used in the experiment was a 4 mm thick sheet. Wire ER5356 (the equivalent of Sv-AMg5) was used as a filler as it is suitable for welding aluminum alloys with magnesium concentration above 3% (AMg3-AMg6). The chemical compositions of alloy AMg4 and wire ER5356 are given in Table 1.

The base metal has a microstructure with grains elongated in the rolling direction and with inclusions of intermetallics  $\text{Al}_3\text{Mg}_2$ , which is typical of sheet materials (Fig. 1).

### 2.2. Experimental methods and equipment

Welding experiments were carried out according to the scheme presented in Fig. 2.

To study how ultrasonic vibrations affect the structure formation of the materials under consideration, the weld

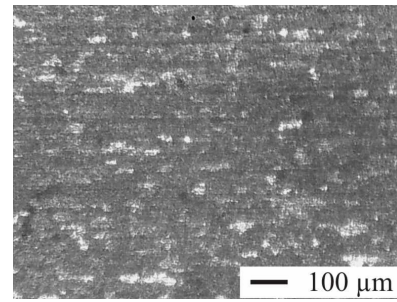


Fig. 1. Microstructure of AMg4 alloy sheet.

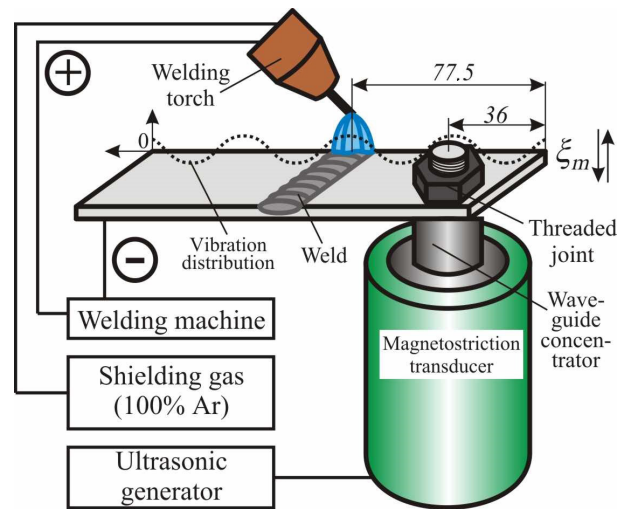


Fig. 2. (Color online) Experimental scheme of welding with ultrasound.

was made on a plate of AMg4 155 × 30 × 4 mm in size while subjecting the plate simultaneously to ultrasonic vibrations.

Before welding, the plate surface was cleaned from oxide film using a disc metallic brush and then degreased.

Welding was done by semiautomatic welding with reverse polarity current and arc shielding, with argon being used as the shielding gas. This type of welding protects melt aluminum from interaction with oxygen and allows removing formed oxides from the surface to be welded.

The MIG 215AL PULSE machine represents a power supply using inverter technology for synergetic energy-pulse bonding. Selecting the aluminum welding program using wire ER5356 0.8 mm in diameter and setting 4 mm thickness of parts to be welded, the following recommended welding parameters were obtained: current  $I_w = 125$  A, wire feeding rate  $V_w = 15.2$  m/min, voltage  $U_w = 22$  V. The argon rate was 17.5 l/min. The weld deposition was 2 s.

To apply vibrations on the plate, a PMS-2,0-22 rod-type double-half-wavelength magnetostriction oscillating system was used consisting of a magnetostriction transducer made of alloy 49K2F placed into a water-cooled housing and a

Table 1. Chemical compositions.

Aluminum alloy AMg4										
Element	Fe	Si	Mn	Cr	Ti	Cu	Be	Mg	Zn	Al
%	<0.4	<0.4	0.5 – 0.8	0.05 – 0.25	0.02 – 0.1	<0.05	0.0002 – 0.005	3.8 – 4.8	<0.2	the rest
Welding wire ER5356										
%	<0.1	<0.25	0.55	0.12	0.12	-	-	5.0	-	the rest

wave-guide concentrator soldered to its end and made of a titanium alloy whose amplifying stage diameter was 30 mm. The waveguide and the plate were connected by a threaded connection via a pin and a nut.

The vibration system was powered by a UZG2-22 generator up to 2 kW. The generator can automatically adjust the frequency and amplitude, which is important to ensure stable vibrations during welding.

Ultrasound was introduced before welding and switched off after achieving the weld temperature of 100°C, which is well below the recrystallizing temperature. Temperature changes were recorded by an IR-thermometer.

One of the most important aspects of welding with vibrations is to find the location on the plate where they should be applied and locate the welding area where the stable ultrasound effect is ensured. This issue was considered in Refs. [16,17,19] where the distance from the source of vibrations to the welding spot was maintained constant, but no justification of the selection of a certain distance was provided.

### 2.3. Determination of vibration application and weld deposition spots

The point of application of vibrations was selected based on the distribution of characteristic vibrations of the plate at a frequency equal to the resonance frequency of the oscillating system  $f = 21800$  Hz. The plate was then covered with sodium hydrocarbonate powder and subjected to ultrasonication so that the powder was distributed on the plate as per that of the vibration amplitude: it is extruded from the antinode zone and accumulated in nodes. From these experiments, a point on a distance of 36 mm from the edge of plate (see Fig. 2), which corresponds to an antinode location, was selected.

The effects of ultrasonic vibrations of three intensities were compared: low-amplitude ( $\xi_m = 3 - 4$   $\mu\text{m}$  for output power of  $W = 200$  W); intermediate ( $\xi_m = 9 - 10$   $\mu\text{m}$ ,  $W = 350$  W), and high-amplitude ( $\xi_m = 13 - 15$   $\mu\text{m}$ ,  $W = 450$  W).

The optimal welding place was selected to be on a distance 77.5 mm from the plate edge, which also corresponds to the antinode zone.

The same dimensions were used during the second stage of the study, i.e. when welding two plates and finding the mechanical properties of joints. The plate was cut in the middle, the plate parts were welded on the edges so that 0.5 mm remained between the plates, with no edge preparation. In these conditions, the vibrations are transmitted to the second plate via welding points along edges and the distribution of the vibrations remains the same. The welding time was 3.5 s.

### 2.4. Defining the structure and properties

After building-up, specimens were cut out of plates for further examination of the surface. The obtained specimens were examined for microstructure, sub-microstructure, and micro-hardness. The specimens were prepared for analysis by pouring with protacryl, with thin sections obtained after its cooling. The microstructure was examined using a METAM RV-22 metallographic microscope. The submicrostructure of surfaces was examined using an SMM-2000 scanning

microscope. The micro-hardness was measured using a PMT-3 microhardness tester. After welding two plates, the obtained joints were examined for deflection caused by metal shrinkage. The joints samples corresponding in size to XII specimens under GOST 6996-66 were tested in tension. These tests were carried out using a UTS-110M-50-0U tensile machine.

## 3. Results and discussion

### 3.1. Analysis of microstructure

The transmission of ultrasound during welding leads to changes in the microstructure in the welding zone (Fig. 3).

The weld joint obtained using a conventional technology has a well-marked boundary between the heat treatment zone in the base metal and the weld metal that has a dendritic structure formed because of growth of crystals from metal grains of the base metal perpendicular to the boundary of fusion deep into the molten pool metal. The width of this zone is 0.84 mm. At a distance from the fusion boundary, the weld metal has a refined structure with grains somewhat elongated in the direction of crystallization.

Joints made by applying ultrasound also have a well-marked fusion boundary in case of significant changes in the weld metal.

In low-amplitude conditions, the microstructure of weld metal has a lot of defects in the form of micro-pores (micro-cracks) shown with arrows in the figure. The location of micro-pores is of relatively regular nature with alternation every 150  $\mu\text{m}$ . The size of the dendritic zone decreases but it is impossible to find where it ends because of the defects. Onward, the weld metal has the same structure.

The microstructure obtained in intermediate conditions has a significantly reduced width of the dendritic zone of 0.33 mm, which is 2.5 times less than in the reference specimen. The weld metal behind this zone has an even structure with insignificantly elongated grains.

Using high-amplitude conditions leads to thinning of dendritic axes without a decrease in their height and to the development of relatively large pores encircled in the figure. The zone marked with a large circle is a fragment of the oxide film with pores formed along the perimeter. Equiaxial grains are formed in the weld metal and high porosity remains.

The obtained changes in microstructure are explained by the effects occurring in liquid metal when ultrasonic vibrations are introduced into the molten pool. Mechanical effects such as sound pressure, cavitation, and acoustic flows of various scales have a significant effect on primary processes of structure formation: energy balance during crystallization, nucleation rate, and nucleus growth rate.

Energy balance for bidimensional nucleus formation in case of heterogeneous spontaneous crystallization writes [20]:

$$\Delta G_{\text{tot}} = 2\pi R h \sigma - \pi R^2 h \Delta G,$$

where  $h$  is the height of the bidimensional nucleus,  $V$  is the volume of the nucleus,  $\Delta G$  is the difference of Gibbs energy of metal in the liquid and solid states,  $\sigma$  is the surface tension between liquid metal and crystalline.



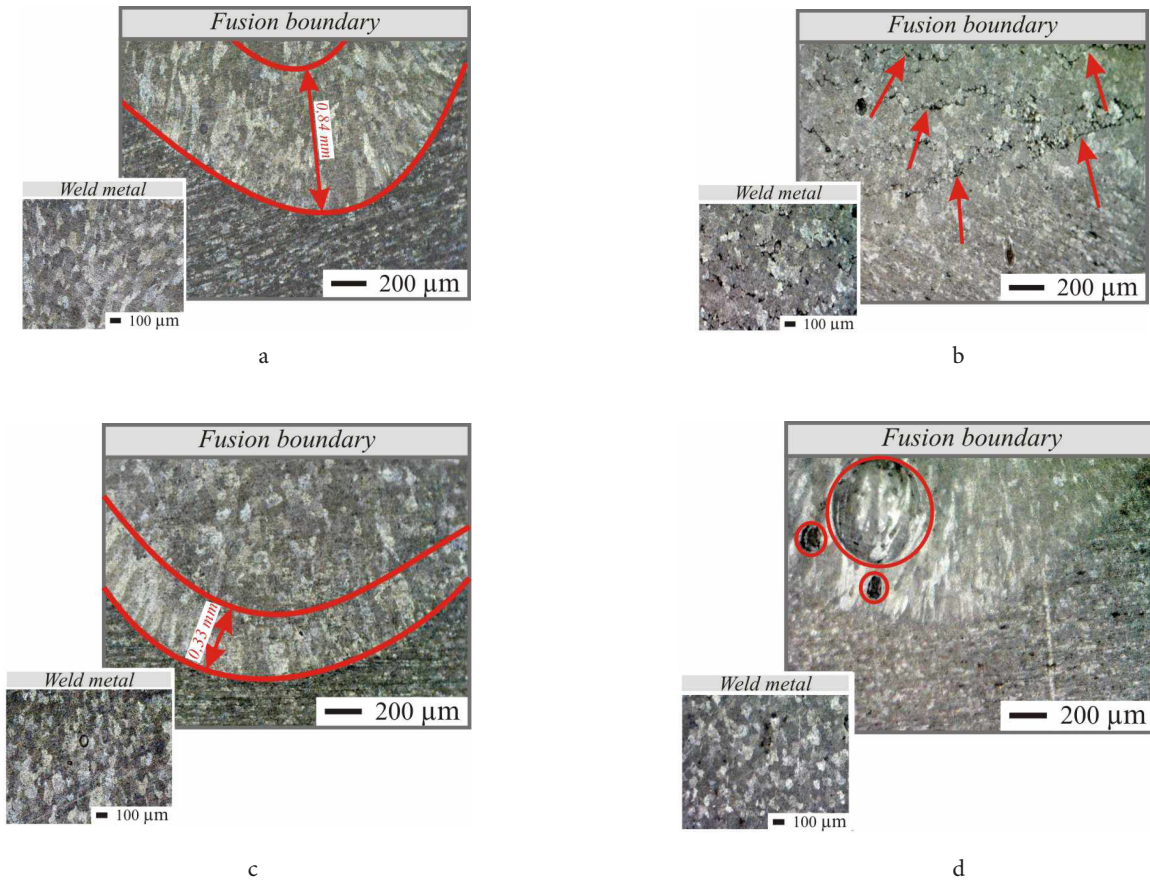


**Fig. 3.** Microstructures of the welding zone without (a) and with applied vibrations:  $\xi_m = 3-4 \mu\text{m}$  (b);  $\xi_m = 9-10 \mu\text{m}$  (c);  $\xi_m = 13-15 \mu\text{m}$  (d).

The critical radius of a nucleus in this case will be:

$$R_{cr} = \frac{\sigma}{\Delta G}. \quad (1)$$

Introducing ultrasound into the molten pool increases the free energy of the system by  $E_{us}$  that is the kinetic energy during the movement of melt molecules under variable sound pressure:

$$E_{us} = \frac{m\vartheta^2}{2},$$

where  $\vartheta$  is the movement speed of molecules:

$$\vartheta = \frac{dx}{dt} = 2\pi f x_0 \cos 2\pi ft,$$

where  $t$  is the time,  $x = x_0 \sin 2\pi ft$  is the vibrations of molecules relative to their middle positions.

The maximum speed will be equal to:

$$\vartheta_{max} = 2\pi f x_0.$$

The initial shift  $x_0$  can be considered as a vibration amplitude of the fusion boundary  $\xi_m$  that is the irradiating surface in this case.

Then:

$$E_{us} = \frac{1}{2} m \omega^2 \xi_m^2.$$

This energy is transmitted to the formed crystallization

nuclei whose mass is as follows:

$$m = V\rho = \pi R^2 h \rho,$$

where  $V$  is the nucleus volume,  $\rho$  is the density.

Then the change in the energy of the system when applying ultrasonic vibrations can be calculated as

$$\Delta G_{tot} = 2\pi R h \sigma - \pi R^2 h \Delta G' + \frac{1}{2} \pi R^2 h \rho \omega^2 \xi_m^2.$$

Differentiating this with by  $R$  and equating to zero:

$$\frac{d}{dR} \left( 2\pi R h \sigma - \pi R^2 h \Delta G' + \frac{1}{2} \pi R^2 \rho \omega^2 \xi_m^2 \right) = 0,$$

one obtains the critical radius for the existence of the center in oscillatory conditions:

$$R'_{cr} = \frac{2\sigma}{2\Delta G - \rho \omega^2 \xi_m^2}. \quad (2)$$

A comparison of Eqs. (1) and (2) shows that introduction of vibrations leads to changes in the maximum size of crystallization nuclei that increases with the amplitude of vibrations. It means that a lower temperature is required for stable formation of nuclei in oscillatory conditions. Increased overcooling and decreased temporary interval of crystallization promote a formation of a fine structure.

A key role in the crystallization process with ultrasound is played by cavitation, which includes the formation, growth, and collapse of bubbles accompanied by a substantial energy release.

Growing dendrites and crystallization nuclei will simultaneously promote the formation of cavitation bubbles and be subject to their effects. When the bubbles collapse, instantaneous pressures and temperatures reach several hundred MPa and several thousand degrees [21]. Such pressures and temperatures lead to dispersion of the formed dendrites and nuclei. Such new nuclei having a radius of  $R > R'_{cr}$  will grow further and serve as cavitation nuclei and the nuclei with a radius of  $R < R'_{cr}$  will melt.

Apart from cavitation, the crystallization process is greatly affected by acoustic flows that promote better mixing of melt components and their movement within the cavitation activity zone. For nuclei moving within the acoustic field, the conditions of bonding of atoms from the liquid molten phase get complicated, which results in decreased growth rate.

The introduction of ultrasound into the molten pool has a comprehensive effect on the crystallization process, which leads to an increased degree of overcooling, increased number of crystallization nuclei, and decreased growth rate.

The differences in microstructures obtained in various vibration conditions are explained by different natures of ultrasound effects depending on the conditions.

For example, low-amplitude conditions are characterized by random small volumes of liquid involved in cavitation and no large-scale acoustic flows. The primary mechanism affecting the structure formation in this case will be the vibration of the fusion boundary retarding the growth of dendrites. The high number of micro-pores is possibly related to the irregular distribution of melt components. The sound wave passing through the liquid metal creates alternating areas with maximum and zero vibrations where gases contained in the melt are accumulated.

In high-amplitude conditions, a high number of cavitation bubbles are accumulated near the irradiating surface accompanied by the absorption of acoustic energy and leading to strong hydrodynamic flows. This results in the elongation of dendrites towards flow directions and promotes the transfer of cavitation bubbles to the molten pool. This explained a higher effect on changes in the weld metal structure at a distance from the fusion boundary. Applying vibrations of high amplitude to the melt can significantly increase the work necessary to form the crystallization nucleus as shown in formula (2) and reduce the temperature of the crystallization start. The high crystallization rate prevents gas bubbles from going on the surface and increases the number of pores.

Intermediate conditions differ by a high cavitation activity concentrated mainly near the fusion boundary and by moderate acoustic flows. Using these conditions when welding AMg4 alloy creates optimal conditions in terms of crystallization kinetics. The share of dendritic segregation falls down significantly in the weld metal.

Further studies of the weld microstructure and weld joint properties were carried out for intermediate treatment conditions.

### 3.2. Analysis of sub-microstructure

Changes in the weld sub-microstructure confirm the suggestions considered above. Figure 4 represents 3D images of surfaces  $308 \times 308$  nm in size obtained by the constant height method when maintains the fixed end of the cantilever at same height

The weld obtained without applying vibrations has steps, which is caused by the layer-by-layer formation of atomic surfaces within the same grain in case of spontaneous crystallization of the melt. The sub-microstructure of a weld obtained with vibrations has almost no traces of layer-by-layer growth, which is caused by the grain refinement. The image probably shows the contact area of several grains having an irregularly shaped surface whose geometry is formed during crystallization in the ultrasound field.

Quantitatively, this is shown by a decreased maximum height of the profile from 91 to 69 nm, almost equal increment of irregularities, and somewhat increased average height of the profile irregularities caused by the action of collapsing and oscillating cavitation bubbles.

### 3.3. Determination of weld joint properties

The obtained changes in the structure on the micro- and sub-microlevel lead to an increased weld joint quality. The distribution of the micro-hardness along a line normal to the fusion boundary is represented in Fig. 5.

For specimens obtained with ( $\xi_m = 9-10 \mu\text{m}$ ) and without vibrations, micro-hardness patterns are obtained to be generally typical of aluminum welding. The weld metal hardness without vibrations is lower below the base metal due to a large dendritic structure, which is followed by a certain reduction in the incomplete mixing zone near the melting boundary and an increase in hardness in transition to the base metal. The micro-hardness pattern obtained with

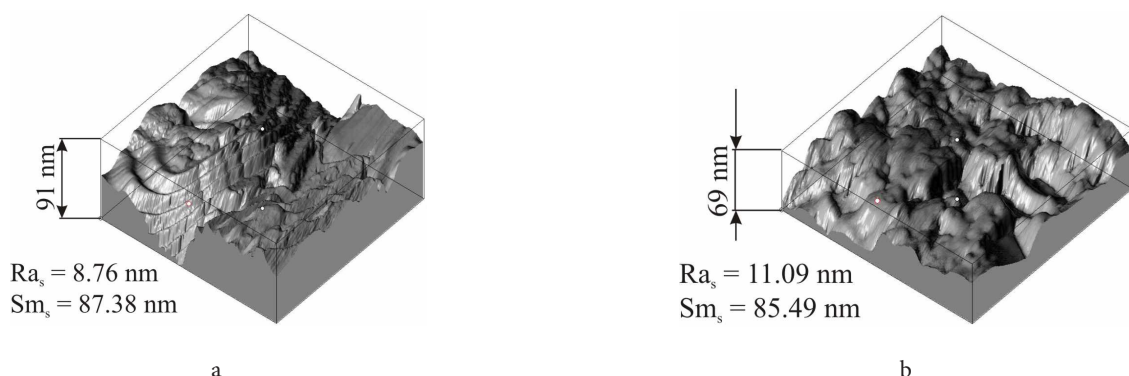


Fig. 4. Submicrostructure of the weld metal: without (a) and with the application of vibrations ( $\xi_m = 9-10 \mu\text{m}$ ) (b).

vibrations is high at a distance from the fusion boundary and then falls down to that of the test specimen in the region from 400 to 300  $\mu\text{m}$ , which corresponds to the transition from the fine structure to the dendritic one. The hardness then remains at the same level and greatly increases after the fusion boundary.

The primary difference in profiles is a smoother transition from the weld metal to the base metal, which shows better mixing of melt components in the fusion zone and leads to the strengthening of the weld joint weak place.

For specimens obtained with oscillations  $\xi_m = 3-4 \mu\text{m}$  and  $\xi_m = 13-15 \mu\text{m}$ , the microhardness of the weld metal is lower than without vibrations, which is associated with structural defects. As a result, the transition to the base metal becomes more abrupt.

Tensile tests of joints (Fig. 6) also show an improvement in the quality of the weld in the optimal mode.

The ultimate strength increased by 5%. The ultrasound had a larger effect on the plasticity of the weld metal whose elongation to failure was 22% higher. For the joint obtained with oscillations  $\xi_m = 3-4 \mu\text{m}$ , the tensile strength and ductility decreased to 10%. With an amplitude  $\xi_m = 13-15 \mu\text{m}$ , the tensile strength is at the control level with a decrease in ductility by 20%.

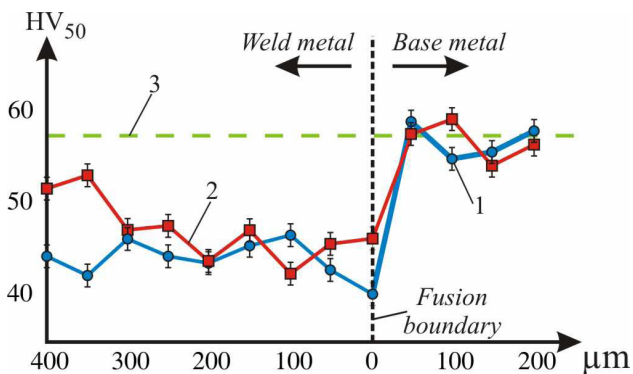


**Fig. 5.** (Color online) Profiles of microhardness of specimens: 1 — without the application of vibrations; 2 — with the application of vibrations ( $\xi_m = 9-10 \mu\text{m}$ ); 3 — control specimen.

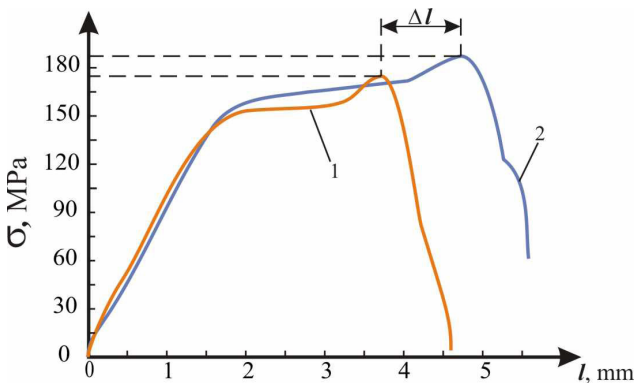


**Fig. 6.** (Color online) Stretch diagram of specimens: 1 — without the application of vibrations; 2 — with the application of vibrations ( $\xi_m = 9-10 \mu\text{m}$ ).

## 4. Conclusions

The theoretical and experimental studies carried out in the present work allow for making the following conclusions:

1. The method of transmitting ultrasonic vibrations to welded elements in a joint can be used during the entire welding cycle (unlike other methods), from forming the molten pool to the complete crystallization of the weld metal.

2. The best results in changing the microstructure of AMg4 alloy weld joints are achieved in intermediate conditions of oscillations. In this case, the weld metal has a regular and fine-grain structure and a 2.5-fold reduced width of the dendritic zone.

3. Introducing ultrasound to the molten pool leads to changes in the kinetics of the crystallization process. The primary parameters characterizing the crystallization, such as overcooling, the number of crystallization nuclei, and their growth rate are changed.

4. Primary mechanisms determining the efficiency of ultrasound are sound pressure, cavitation, and acoustic flows. Cavitation provides dispersion of the nuclei (mainly, growing dendrites) and retards their growth rate. Acoustic flows provide for even mixing of melt components and transfer nuclei to cavitation activity zones.

5. The analysis of sub-microstructure confirms the changes in the crystallization process. Grains obtained with vibrations have no traces of spontaneous crystallization shown by steps of helical dislocation.

6. The weld joints obtained by applying ultrasonic vibrations have an increased strength and high plasticity.

*Acknowledgments.* This research was funded by the Russian Science Foundation, grant number No. 21-79-00185, <https://rscf.ru/project/21-79-00185/>

## References

1. S.K. Sundukov, R.I. Nigmatzyanov, D.S. Fatyukhin. Russian Metallurgy (Metally). 13, 29 (2021). [Crossref](#)
2. H.K.D.H. Bhadeshia. Science and Technology of Welding and Joining. 20 (6), 451 (2015). [Crossref](#)
3. D.M. Ryabkin, A.V. Lozovskaya, I.E. Sklabinskaya. Monografiya: metallovedenie svarki alyuminiya i ego splavov. Kiev (1990) 160 p. (in Russian)
4. R. Xiao, X. Zhang. Journal of Manufacturing Processes. 16 (2), 166 (2014). [Crossref](#)
5. E. Sh. Statnikov, V.O. Muktepavel. Welding International. 17 (9), 741 (2003). [Crossref](#)
6. S.K. Sundukov, R.I. Nigmatzyanov, V.M. Prihod'ko et al. Russian Engineering Research. 41 (6), 570 (2021). [Crossref](#)
7. Y. Han, et al. Mater. Sci. Eng.: A. 405 (1-2), 306 (2005). [Crossref](#)
8. V.I. Dobatkin, G.I. Eskin. Proc. 4th Int. Conf. on Semi-Solid Processing of Alloys and Composites. Univ. Sheffield, UK (1996) p. 193.
9. Patent USSR № 515608/30.05.1976. (in Russian)
10. Q. Sun, et al. China Weld. 17 (4), 52 (2008).
11. Y. Y. Fan, C. L. Yang, S. B. Lin, C. L. Fan, W. G. Liu. Weld. J. 91 (3), 91 (2012).

12. Y. Cui, C. Xu, Q. Han. *Advanced Engineering Materials*. 9 (3), 161 (2007). [Crossref](#)
13. C. Zhang, M. Wu, J. Du. *Tsinghua Science and Technology*. 6 (5), 475 (2001).
14. T. V. da Cunha, C.E. Niño Bohórquez. *Ultrasonics*. 56, 201 (2015). [Crossref](#)
15. G.I. Eskin. *Ultrasonic Sonochemistry*. 8, 319 (2001). [Crossref](#)
16. H. Dong, et al. *Mater. Sci. Eng.: A*. 534, 424 (2012). [Crossref](#)
17. X. Cai, S. Lin, X. Wang, C. Yang, C. Fan. *Materials*. 12, 4081 (2019). [Crossref](#)
18. C. Chen, C. Fan, Z. Liu, X. Cai, S. Lin, Y. Zhuo. *Acta Metall. Sin. (Engl. Lett.)*. 33, 1397 (2020). [Crossref](#)
19. Q. Chen, S. Lin, C. Yang, C. Fan, H. Ge. *Acta Metall. Sin. (Engl. Lett.)*. 29, 1081 (2016). [Crossref](#)
20. *Teoriya svarochnyh processov: uchebnik dlya vuzov po spec. "Oborudovanie i tekhnologiya svarochnogo proizvodstva"* (ed. by V.V. Frolov). Moscow (1988) 559 p. (in Russian)
21. D.S. Fatyukhin, R.I. Nigmatzyanov, V.M. Prikhodko, A.V. Sukhov, S.K. Sundukov. *Metals*. 12 (138), (2022). [Crossref](#)